STRUCTURAL AND RHEOLOGICAL ASPECTS OF SOME IONIC AND COVALENT GLASS-FORMING MELTS

Animesh Jha, M. Naftaly, and V. Tikhomirov
Department of Materials, University of Leeds, Clarendon Road, Leeds LS2 9JT.

ABSTRACT

The structure of a glass largely determines its properties. In the present investigation, we compare the low (Boson) and high (optical) phonon spectroscopic data for selected fluoride, chalcogenide and heavy-metal oxide glasses, namely fluoroaluminates (AlF_3-M $(Ba,Ca)F_2$-YF_3), fluorozirconates (ZrF_4-BaF_2-NaF), GeS_2, As_2S_3, Ga_2S_3-La_2S_3, and binary and ternary TeO_2 glasses. The structural significance of Boson peak (low frequency acoustic phonons) and high-frequency optical phonons is explained in view of the thermal and crystallisation properties of glass. Based on the Boson peak analysis, the magnitudes of short and medium-range order in these glasses are compared. On the basis of the extent of medium range order, the structural origin of excess free volume in a glassy structure is defined and its role in determining the viscosity of a glass is explained.

INTRODUCTION

The short-range order structure of glasses have been studied by numerous techniques, namely the neutron diffraction, EXAFS, small-angle X-ray scattering, magic angle spin NMR, X-ray photoelectron spectroscopy, and the vibrational spectroscopic techniques. Each of the above techniques has its advantages and limitations, and in many ways the use of a combination of above techniques for structural analysis of a glass provides a more detailed understanding of its structure. The spatial resolution of atoms or ions in a glass structure is dependent on the technique adopted[1]. For example, in the neutron diffraction experiments, neutrons are scattered by nuclei and yield data for the spatial distribution of nuclei[2]. By comparison, in the X-ray diffraction studies, the electrons contribute to the scattering and, it is assumed that each electron in the structure can be associated with a particular atom during the interaction time of given X-ray photon. The Fourier transform of the interference pattern from X-ray scattering yields a poorer spatial resolution data for atomic positions than in neutron diffraction[3]. A much better structural data in terms of the bond distance and co-ordination number are derived in EXAFS techniques than in the diffraction techniques. In general, the two diffraction techniques together with EXAFS spectroscopy reveal a more complete information than the data from the individual techniques[4].

Most of the vibrational spectroscopic studies using the Raman and IR reflection spectroscopy have been concentrated to analyse the dominant vibrational modes in the high-energy part of the spectra (> 200 cm^{-1}) in oxide[5], fluoride[6-7] and sulphide glasses[8]. Using the vibrational spectroscopic data for crystal analogues of such glasses, structural models have been developed[1,6,7]. The models based on vibrational spectroscopic analysis of glass structure are generally consistent with EXAFS spectroscopy, NMR and diffraction techniques, for example, for fluoride and oxide glasses[9].

The short-range order (SRO) exists in crystalline solids, glasses and in their corresponding liquids. The molar volume of a silica glass, for example, falls between the liquid at high temperature and the crystalline quartz state. The presence of medium or intermediate range order (acronymed hereafter as MRO) in the glass has been indirectly inferred on the basis of the interpretation of the specific heat, coefficient of thermal expansion and density of glasses. However there is still a major lack of understanding of the MRO in various glasses, in particular the fluoride, halide and sulphide glasses described below. As discussed above the diffraction and spectroscopic techniques are limited in spatial resolution up to 0.4 nm maximum, no direct evidence for MRO in glasses can be obtained by adopting the above analytical techniques directly.

More recently the Raman spectroscopic technique has been adopted by a number of researchers[10-17]. The presence of the Boson peak (BP), which appears in the low frequency part of Raman and depends on the glass compositions, has been found to be a ubiquitous feature of the amorphous structure. The existence of BP is supported by a soft-potential model[17], which explains that the Bosons are quasilocal vibrational modes at low frequencies, and follow the reduced mass (μ) - linear harmonic oscillator (υ_o) relationship. For example, it has been suggested[17] that in selenium glass that these soft modes atomic chains and rings have effective masses of twenty atomic masses or so. The clustre-like structural description may possibly explain the regions of discontinuity in the glass structure, as the phonons may be damped or scattered from such structural inhomogeneities. The regions of discontinuity has connotations with model proposed by Duval and co-workers[18], in which the authors considered random non-continuous networks as if they were nano-crystalline regions. By analysing the Boson peak in each glass, described herein, it may therefore be possible to

identify the origin of molar free volume quenched in the vitreous state and develop a better physical description of the structural origin of Bosons i.e. the acoustic phonons.

In this paper, we present a detailed structural interpretation of the BP and, in particular, the position of the Boson peak and its intensity increase are described. By using the velocity of sound in glassy media described below, the acoustic phonon mean free path lengths ($?_B$, nm, which is equivalent to SCL in the Martin-Brenig Model[19]) have been derived. Furthermore we have used the measured viscosity and coefficient of thermal expansion data for determining the molar free volume present in the glass above and below its glass temperature respectively, which is then expressed semi-quantitatively in terms of the configurational entropy. The difference in the molar free volume below and above T_g reveals the origin of rheological behaviour of glass-forming melts.

Finally based on the characterisation of structural discontinuity, determined by phonon mean free path length using the Martin-Brenig (MB) model[19], we present a relationship between the molar free volume and structural discontinuity, which arise due to the non-bridging sites in the glass structure. It is anticipated that such an understanding and characterisation of non-bridging sites in the glass structure is crucial for developing a greater understanding of polarizability, viscous flow and charge transport paths in the glass. For understanding the effect of polarizability, we have chosen different types of host glasses, and lanthanides as dopant ions.

EXPERIMENTAL

Fluoride glass compositions, described in **Table 1**, were made by melting the mixtures of starting powder in a relatively moisture-free atmosphere. Fabrication of bulk fluorozirconate (ZBLAN) and aluminium fluoride (AlF_3) based glasses require dry and partially oxidising atmosphere for melting. Whereas the gallium fluoride (GaF_3), indium fluoride (InF_3), cadmium mixed halide (CdFCl) and silver iodide (AgI) based glasses must be melted in a dry and inert atmosphere. An extremely dry atmosphere inside the melting chamber is essential for maintaining the transparent quality of cast GaF_3 and InF_3 glasses. The characteristic pouring and annealing temperatures for each glass is reported in ref[20]. Each glass was cast into a 3 mm thick brass mould by quenching the melt from the pouring temperature. The quality of glass was determined by examining the presence of crystals in an optical microscope. In general, it was found that most glasses can be cast into rods up to 12 mm in diameter and 100 mm in length except for AgI-based glasses, for which the maximum thickness was limited to 3 mm. The quality of the fluoride glasses also depend on the purity of the starting materials[21a] and, due care was exercised to avoid incorporation of oxide and oxygen-bearing impurities such as OH^- and nitrates etc., which contribute to extrinsic light-scattering centres in the glass. After casting halide glass samples, the samples were polished for Raman spectroscopic measurements.

Chalcogenide glasses, on the other hand, were made in sealed silica ampoules[22], as the vapour pressures of chalcogenide compounds are significant at the melting temperatures. High vapour pressure invariably leads to the loss of materials from the surface of the melt, when a chalcogenide glass is melted in an unsealed container. The use of sealed silica ampoules for melting chalcogenide glasses also helps excluding the atmospheric oxygen during melting. After melting and homogenisation above 1000°C, the ampoule containing chalcogenide liquid was quenched to room temperature.

Polished samples of glasses were prepared for spectroscopic and thermal analyses. The characteristic temperatures for each glass were determined by differential thermal analysis (DTA) and differential scanning calorimetric (DSC) techniques, whereas the coefficient of thermal expansion and flow behaviour were determined by dilatometric and rheometric techniques, described elsewhere[20,22]. Raman spectroscopic analysis on polished glass samples was carried out using a double grating

monochromator with spectral resolution of 1.5 cm^{-1}. The excitation wavelength for Raman emission was 647 nm line of Kr^+ laser, or the 515 nm line of Ar^+ laser. Infrared and uv-visible spectra were analysed using Perkin-Elmer FTIR and Lamda-19 spectrophotometer. Both spectrophotometers use a double-beam source for correcting the reflection loss in the total absorption measurement experiments.

RESULTS

The Raman and infrared reflection spectroscopic techniques are two complementary methods for analysing the vibrational modes in an amorphous structure[24]. In the Raman technique, the incident photon (λ_p) is inelastically scattered by the transverse optical (TO) modes in the glass matrix. The scattered or emitted photon, which is the result of phonon excitation, could be either to a lower (Stokes line) or to a higher (anti-Stokes line) energy. The microscopic excitation process in infrared reflection and Raman are quite different. The vibrational modes are only Raman-active when they are associated with a change in the polarizability, as opposed to the change in the dipole moment for IR transitions. The vibrational modes, which are centro-symmetric (i.e. the breathing modes) are **Raman-active**, whereas the non-centrosymmetric modes are **IR-active.** In the glassy state both modes are observed due to the amorphous nature, it is due to the existence of both modes that IR reflection and Raman spectroscopic techniques prove useful in the analysis of the glass structure[24]. The dominant Raman peak (ν_o, cm^{-1}) in each glass is plotted against the reduced mass [$\mu=(m_1.m_2)/(m_1+m_2)$] in **Figure 1**, which is a linear harmonic oscillator relationship. In this figure, we have also plotted the value of cation-anion distance (nm) as an indirect measure for determining the force constant, *f*, upon which the value of ν_o also depends as shown in eq.1.

$$\nu_o = \frac{1}{2\pi}\sqrt{\frac{f}{\mu}} \qquad (1)$$

Using Kr^+ and Ar^+ ion source wavelengths, the Raman spectra for various fluoride, sulphide and heavy metal oxide and fluoride glasses were studied. Both lanthanide (Ln^{3+})-doped and undoped samples were investigated. The spectra shown in **figures 2a** to **2e** are for fluoroaluminate, TeO_2, GeS_2-based, gallium-lanthanum sulphide (GLS) and As_2S_3 glass compositions respectively. The high frequency (optical phonon) region of each spectrum has more than one peak, which are assigned to structural symmetric vibration modes (ν_R, cm^{-1}). The most dominant peak for each glass is assigned to the symmetric stretching of the structural unit e.g. say SiO_4 tetrahedral breathing mode near 1120 cm^{-1}, GeS_4 and TeO_4 tetrahedral symmetric stretching modes at 345 cm^{-1} and 780 cm^{-1} respectively, see **Table 2**. Because of the smaller polarizability of Al^{3+} ions, the Raman spectrum for AlF_3 based glasses is weak and the peaks are less resolved from background noise.

The spectra in **figures 2a** to **2f** show BPs, which is an important common feature in all the glasses reported in this paper. As referred above by Gurevich et al[17], that BP in glasses are due to quasi-local vibrational modes. In glasses such modes or the origins of structural discontinuity, as reported in Se[25], are likely to be non-bridging structural sites where the acoustic phonons encounter dampening and/or scattering. Below we have analysed BP in **Figures 2a to 2f** and also qualitatively described a relationship with fractional molar free volume in fluoride, heavy metal oxide and sulphide glasses with the acoustic phonon mean free path length determined from the MB theory. In this context, some BP data from literature have also been reviewed[11-14].

Recently an investigation was carried out by McIntosh co-workers[13] on vitreous silica and alkali-modified silicates. The authors reported three important features in the Raman spectra of alkali-modified silicates. The frequency of BP followed the harmonic oscillator relationship as shown in equation 1 when plotted against the reciprocal mass of the cations incorporated for the modification of the silica glass structure. McIntosh and co-workers reported that the relative intensity of Boson peak does not change significantly with the size of cations present in the silicate structure. However, the frequency of BP varied between 486 cm^{-1} for Cs^{1+} ions containing glass, and 539 cm^{-1} for sodium containing glass. Another important feature of silica glass structure is that a "broad band" was observed. Galeener[26] assigned the broad band to the Si-O-Si bending modes, the intensity of which would be expected to decrease as the number of non-bridging oxygen (nbo) bonds in the structure increases. The nbo bonds are produced as the alkali concentration in the glass increases. The reduction in the intensity of "broad band" was also interpreted as an indicator of the reduced structural connectivity. The presence of "broad band" is a unique feature of silica and to a lesser extent of modified silicate glasses. We find in **figure 2c** that there is also the strongest evidence for a broad band in each family of GeS_2 glass. However in other spectra (**Fig.2a, 2b, 2d and 2e**), the evidence is rather weak.

From the results presented in Figures 2a through 2f, it is evident that highly polarisable rare-earth ions enhance the intensity of the BP, and the extent of enhancement of the BP intensity is dependent on host. After reaching a concentration, called the saturation concentration, the intensity of BP does not increase. The intensity of BP therefore depends on the polarizability of both the host glass network ions andity and the dopant ions, e.g. rare-earth ions discussed above.

We have compared the depolarisation ratio (I_{VH}/I_{HH}) from ref[27] which points out that the maximum value of depolarisation ratio (Φ) is 0.6 for the BP in $Ge_{0.345}$-$S_{0.55}$-$I_{0.10}$ glass, for example. The values of Φ corresponding to a minimum at 100 cm^{-1}, 225 cm^{-1} and 345 cm^{-1} frequencies are for symmetric vibrational modes. The analysis of depolarisation spectrum in Ge-S-I glass points out that the "broad frequency band" at 100 cm^{-1} may be similar to that observed in silica glass.

DISCUSSION

Analysis of low frequency Raman spectra

The frequencies of BP in oxide, halide and sulphide glasses are plotted against the reduced mass in **Figure 4 (see Table 2)**, from which we find eq.1 is not followed. This observation is in contrast with the results presented for the BP in alkali-modified silicate glasses by McIntosh co-workers[13], which may suggest that for the analysis of BP, eq.1 may only be restricted to a specific family of glasses and the relationship cannot be extended beyond a given family. By examining the Boson peak results for glasses discussed herein and by reviewing the results reported in the literature[11-14], the following conclusions for undoped and RE-ions doped glasses can be drawn.

a) In a strong covalent (undoped) glass, e.g. silica or B_2O_3, has a BP at a lower Raman frequency than 50 cm^{-1} and they are weak due to the smaller polarizability of cations. The intensity of BP also depends on the density of states, which may also be related with the number of non-bridging sites per unit volume of the glass, which are much smaller in silica and B_2O_3 compared

to other types of moderately covalent glasses such as GeS_2, TeO_2 and As_2S_3 glasses. In GeS_2, As_2S_3 and TeO_2 glasses, the Boson peaks are also at low frequencies (< 50 cm^{-1}) and have strong intensities due to the high polarizability of cations such as Ge^{4+}, As^{5+} and Te^{4+}.

b) The Boson peak in ionic glasses such as fluoroaluminate[14] and fluorozirconate[12] glasses is weak due to the small polarizability of cations coupled with fluorine anions (cf. metal-sulphur pairs in chalcogenides). Consequently the intensity of BP is weak (see **figure 2a**). The ionic chalcogenides such as GLS have a comparatively more intense BP than fluorides, however it is weaker than moderately covalent chalcogenides because of the polarizability of S^{2-} ions in GLS is higher than F^- in fluoroaluminate and fluorozirconate glasses.

c) By comparing the full width of half maximum (FWHM) of BP in AlF_3, GLS and Ge_2S_3 glasses, we find that the higher the ionicity of a glass, the greater is the FWHM. The width of BP may therefore mean that there may be more than one type of regions of structural continuity, at the boundary of which the quasi local phonons may have characteristically different energies. Therefore a broad Boson peak may represent multiple potential wells for quasi local phonons. The observation on the breadth of the BP in ionic glasses is consistent with the narrowness of BP in strongly covalent glasses, such as GeS_2-Ga_2S_3, GeS_2-Ga_2S_3-CsI, Ge-S-I, TeO_2 and As_2S_3 glasses in **Figures 2b, 2c and 2e** respectively. On the basis of the results presented in this paper, we present a schematic illustration in **Figures 5a and 5b** to explain the origin of quasi local phonons in the ionic and covalent glasses respectively.

The above conclusions (a) and (b) are based on a structural approach that the phonons which contribute to Boson peak are local and represent structural discontinuities. By comparing the density of a glass with the parent crystalline phase, e.g. v-silica with quartz, the number of structural discontinuities, which defines the molar free volume in a given glass, is far fewer than the interconnected structures. The relative weakness of the Boson peak intensity in silica suggests that there are comparatively smaller number "Boson-active" sites (discontinuous regions or units) in silica than in other types of glasses known in the literature. In silicate glasses[13], the depolarisation ratio (Φ) of BP increases with increased cation mass, and it was also found to be varying with quenching and annealing conditions. Such a variation of Φ may be expected because of the change in topological configuration of modifying cations at the non-bridging sites with the annealing temperatures in the silicate glass. On the other hand, in fluorozirconate and fluorohafnate glasses[12,14], the values of Φ does not change substantially either with the temperature or with the frequency between 20 cm^{-1} and 300 cm^{-1}. The authors in ref.12 reported that ZrF_4 and HfF_4 based glasses were more fragile because of the lack of the structural connectivity. The lack of broadband is more conspicuous in fluoride glasses than in covalent glasses. As explained by Galeener[26] that the two SiO_4 tetrahedra are connected via Si-O-Si bonds and the bending mode of this bond gives rise to a broad band. The evidence for a broadband feature in the BP spectra of silicate glasses may therefore help disclosing the origin of the structural fragility and strongly nonlinear temperature dependence of rheological flow behaviour of other types covalently and ionically bonded glasses such as the chalcogenide family and the halide glass family. The presence of a broad band appears to be true for the Ge-S-I glass, in which there is also a strong evidence for "broad frequency band", which has a symmetric vibration mode (see **figures 2a-2e**).

A Relationship Between Molar Free Volume, Boson Peak And Acoustic Phonon Mean Free Path Length (?$_B$)

The rheological behaviour of a glass is explicable on the basis of the free-volume model, suggested by Doolittle[29]. The main difference, as we understand, between a crystal (e.g. quartz) and a glass (e.g. SiO_2) is the presence of excess free volume in the structure, gwhich is distributed randomly in a glass. By contrast, the long-range periodical order does not permit randomness in crystals. The entropy

$$\Delta S_{tot} = \int \Delta C_p . d(lnT) \qquad 2$$

associated with the free volume change can be determined by carrying out a slow isochronal experiment to determine the specific heat change at T_g using a differential scanning calorimeter. The entropy change then can be given equation 3. The specific heat changes for some fluoride glasses are given in Table 2.

The vibrational spectroscopic analysis, discussed above, has revealed that the origin of Boson peak in a vitreous phase can be ascribed to an environment of non-bridging bonds. Note that the Boson peak is a universal characteristics of a glass structure. As discussed above, the relative intensity of "broad band" peak determines the structural connectivity of tetrahedra in silicate glasses. It is therefore relevant to propose that the "Boson-active sites", which are due to non-bridging bonds, and the molar free volume are likely to be the same in a glass structure, except with one major difference. It is likely that not all non-bridging sites, which defines the molar free volume in glass and glass-forming melts, are occupied by polarisable ions; thereby do not give rise to efficient ligand coupling that enhances the intensity of Boson peak. However the non-bridging sites unoccupied by polarizable ions do participate in the structural rearrangement and relaxation processes. There are many indirect supporting evidences for distinguishing the occupied and unoccupied non-bridging sites in the literature. For example, when RE ions are added in fluorozirconate and fluoroaluminate glasses, the glass transition temperature, T_g, rises with the concentration, making the overall structural relaxation process slow.

Santos and Almeida[11] studied the short and medium range order in zinc halide glasses. It was reported that above the glass transition temperature (T_g), the Boson peak intensity increased consistent with the temperature dependence of the Bose factor, n(ω,T) i.e.

$$I_R = \frac{I_\omega}{[n(\omega,T)+1]} \qquad \textbf{(3)}$$

where n(ω,T) defines the Bose factor and is equal to

$$n(\omega,T) = [\exp(\frac{h\omega}{\kappa T})-1]^{-1} \qquad \textbf{(4)}$$

The BP was also found to be broader with increasing temperature, which means that within a broad peak, there is a distribution of Boson, and increasing the temperature increases the polarisability of such Bosons. The smaller the Boson distribution the narrower the peak becomes. The peak wavelength is therefore an indication of average distribution of Bosons in a glass structure.

Using the acoustic velocity data ($\mathbf{V_{ac}}$) in ref.[11], the phonon mean free path length ($?_B$) were determined for comparing the extent of MRO in various glasses. The magnitude of $?_B$ (nm) was calculated from the MB theory[19] and summarised below in **Table 2**. It can be concluded that the larger is the value of $?_B$, the smaller is the molar free volume at T_g and, therefore the smaller is the number of degrees of freedom for maintaining the viscous flow. It is therefore possible to deduce that the glasses with larger values of $?_B$, (smaller value of V_{Tg}) are likely to manifest a much higher viscosity than those glasses having shorter phonon mean free path length. In **Table 3**, we have also compared the value of a $V_{Tg} = \alpha_v.T_g$ product, where α_v which is a measure of the fractional molar free volume in the glass at the onset of T_g (or the volume expansion coefficient). The relationship between MRO and V_{Tg}, discussed above, points out to several interrelated properties of a glass, and explains the scale of structural relaxation during the annealing of glass above and below T_g. Furthermore the magnitude of $?_B$ explains the origin of internal surfaces in the glass, which determine to the dynamics of relaxation, the rate being slower with larger values of $?_B$, enabling such glasses to become more resistant to devitrification and crystallisation.

The Temperature Dependence of Viscosity

Using the Doolittle equation 4[29], the temperature dependence of viscosity was derived by Ramachandra Rao et al[30] which was based on the Eyring hole theory[31]. Subsequently it was shown[32] that the Eyring model can be employed to express the viscosities (η, Pa s) of halide melts in the range spanning over T_g and the melting point. In **Figures 6**, we have compared the viscosities of silica, BeF_2, a GeS_2-based glass and a fluorozirconate glass, which is acronymed as ZBLAN[32]. The steepness of the viscosity curve on the normalised temperature scale (T/T_g) is an indication that the free volume change is associated with the corresponding change in viscosity. The slope of η vs T_g/T curve for a ZBLAN glass near T_g is much greater than in other types of glasses compared in Figure 6. A similar temperature dependence of η was observed for AlF_3 and CBN-Ph compositions and these are reported elsewhere[20]. The rate of the change in the molar free volume as a function of temperature could therefore be used as a measure for the structural fragility[33] of glass, where the molar free volume, $V_f = C.\exp(-\Delta H_h/RT)$ and the slope dV_f/dT is equal to $(\Delta H_h/RT^2).V_f$. The temperature dependence of molar volume can be estimated from the Eyring equation for halide melts, whereas for covalent glasses the molar free volume can be calculated from the Vogel-Fulcher equation[32]. The temperature coefficient of viscosity for silica, GeS_2 and BeF_2 glasses is independent of temperature, see **Figure 6**, whereas for fluoride glasses, the viscosity changes rapidly with temperature. The lack of structural connectivity in fluoride glasses is responsible for their lower viscosities than in silicates and other covalently bonded melts. The BeF_2 glass apparently behaves very much like silica rather than a ZBLAN glass. The reason for this behaviour between silica and BeF_2 is the structural rigidity of BeF_4 tetrahedra, which is comparable with SiO_4 tetrahedra between T_g and melting point. Unfortunately there are no BP data for BeF_2 glasses to compare.

Finally, we have computed the total molar free volume (V_f) using the viscosity data at T_g based on the Eyring model (see **Table 3**) and compared V_f with the corresponding value of V_{Tg}. The values of V_f at T_g is higher than V_{Tg} for each glass. In Table 3, the values of V_{Tg} for all fluoride and halide

glasses calculated from the $\alpha_v.T_g$ relationship is very nearly 0.025, which is consistent with the assumption described in ref.32. The equation for f_T are given in Table 3. The physical meaning of V_{Tg} can be attributed to the thermal dilation of the structural unit, whereas V_f is due to the configurational changes as well. In other words, the values of V_f and V_{Tg} designate the fractional volume change above and below T_g respectively. V_f therefore takes into the volume change at the melting point, as it is derived from the fitted viscosity equation. The difference (V_f-V_{Tg}) is clearly in agreement with the specific heat change at T_g for glasses known in the literature. The value of fractional molar volume change at the melting point for fluorides is approximately 0.35 and for glasses that exhibit largely a linear relationship[34] on a log η vs $1/T$ graph is 0.07[32]. The difference between the fractional molar volume below and above T_g, from the Adam-Gibbs equation[35], proportionately defines the excess configurational entropy available for the viscous flow of glass above T_g. It is therefore important to note that the glass above T_g is at a configurationally different state than below T_g.

The magnitude of frozen-in state (V_{Tg}) is also important for defining the viscous flow. The higher the value of V_{Tg}, the greater is tendency for flow above T_g, as the bonds become weaker. This is the reason that the fluoride glasses, such as ZBLAN, CBN-Ph, AlF_3-126 and InF_3-1, have a higher value of V_{Tg} than the silicate and GeS_2 glasses, which consequently explains the origin of high viscosity in covalent glasses.

CONCLUSIONS

The observations made via the Raman spectroscopic technique are consistent with the determination of IR cut-off edge. The intensity of a Boson peak is strongly dependent on the cation polarizability and phonon coupling at the non-bridging sites.

The presence of "broad band" in glass is a strong indication for the structural continuity in glass. The breadth of BP in ionic glasses is larger than in covalent glasses, the larger width may therefore represent the multiplicity of the regions of structural discontinuity with unique vibrational frequency signature.

The molar free volume, which defines the viscosity of a glass, is related with the non-bridging structural sites. Such sites are also Boson-active sites and contribute to the intensity of the Boson peak. A non-bridging site can therefore be distinguished by identifying them with or without a resident polarisable ion. The structural correlation length is inversely related with the fractional molar free volume at T_g. The Boson-active sites are the vibrational representation of the molar free volume in the glass. The covalent glasses, discussed above, have lower values of V_f, V_{Tg} and V_f-V_{Tg} than the heavy metal fluorides such as ZBLAN, InF_3-1 and AlF_3-126 glasses. The difference term (V_f-V_{Tg}) is a representation of configurational entropy for the flow of glass above T_g.

REFERENCES

[1] J. H. Simmons, C. J. Simmons, R. Ochoa and A. C. Wright: *in* Fluoride Glass Fibre Optics, ed. I. D. Aggarwal and G. Lu, Academic Press (1st edition), 1991, P.53.

[2] A. C. Wright, J. Non-crystalline Solids, **75**, 15, (1985).

[3] T. M. Hayes and A. C. Wright, *in* Structure of Non-crystalline Materials, ed. P. H. Gaskell, J. M. Parker and E. A. Davis), Taylor & Francis, London, UK, pp. 108-119, 1982.

[4] G. N. Greaves *et al*, *in*, Recent Developments in Condensed Matter Physics, Plenum N. Y. p.225 (1981).

[5] F. L. Galeener, J. Non-crystalline Solids, **49**, 53 (1982).

[6] C. M. Baldwin and J. D. Mackenzie, J. Non-crystalline Solids, **31**, 441-5 (1979), J. Am. Ceram. Soc. **62**, 537-8 (1979b).

[7] C. M. Baldwin, R. M. Almeida and J. D. Mackenzie, J. Non-crystalline Solids, **43**, 309-344 (1981).

[8] G. Lucovsky et al: Phys. Rev. B, **10**, 5134 (1974).

[9] J. Wong and C. A. Angell: *Glass Structure by Spectroscopy*, Marcel Dekker, N.Y., 1st edition 1976, **a). pp. 409-496, b). pp. 669-698, c). pp. 53-88.**

[10] R. M. Almeida and J. D. Mackenzie: J. Mater. Sci., **17**, 2533 (1982).

[11] L. F. Santos and R. M. Almeida: J. Non-crystalline Solids, **232-234**, 638-643 (1998).

[12] J. Schroeder, M. Lee, S. K. Saha and P. D. Persans: ibid, **222**, 342-347 (1997)

[13] C. McIntosh, J. Tolouse and P. Tick: ibid, **222**, 335-341 (1997).

[14] V. Tikhomirov et al: J. Non-crystalline Solids 1999 (in press)

[15] A. A. Kharlamov, R. A. Almeida and J. Heo, J. Non-crystalline Solids, **202**, 233 (1996).

[16] V. K. Malinovsky and A. P. Sokolov, Solid State Commun, **57**, 757 (1986).

[17] V. L. Gurevich et al: Phys. Rev. B, **48**, 16318 (1993).

[18] E. Duval, A. Boukenter and T. Achibat: J. Phys.: Condens. Matter **2**, 10227 (1990).

[19] A. J. Martin and W. Brenig, Phys. Stst. Sol. B **64**, 163 (1974).

[20] M. Naftaly et al: ibid **213 & 214**, 106 (1997).

[21] J. M. Parker and P. W. France: in *Glasses and Glass Ceramics*, ed. M. H. Lewis, Chapman & Hall, 1989, London, **a). P. 162, b). P.176.**

[22] D. Marchese and A. Jha: J. Non-Crystalline Solids, **213 & 214,** 382 (1997).

[23] D. R. Simmons et al: ibid, **185**, 283 (1995).

[24] S. R. Elliott: Physics of Amorphous Materials, Longman Scientific & Technical, Harlow, 1984, P. 153.

[25] H. R. Schrober, C. Oligschleger and B. B. Laird, J. Non-crystalline Solids, **156-158** , 965 (1993).

[26] F. Galeener, Phys. Rev. B, **29**, 4292 (1979).

[27] V. Tikhomirov et al: Solid state Comm. 1999 (in press)

[28] A. F. Wells: Structural Inorganic Chemistry, Clarendon Press, Oxford, 3rd Edition, 1962, P. 526.

[29] A. K. Doolittle: J. Appl. Phys. **22**, 471 (1951).

[30] P. Ramachandra Rao, B. Cantor and R. W. Cahn: J. Material Sci. **12**, 2488 (1977).

[31] N. Hirai and H. Eyring: J. Appl. Phys. **29**, 810 (1958).

[32] A. Jha and J. M. Parker: Phys. Chem. Glasses, **30**, 220-228 (1989).
[33] C. A. Angell: J. Non-crystalline Solids, **73** 1 (1985).
[34] M. Hemingway and A. B. Seddon: ibid **161**, 323-326 (1993).
[35] G. Adam and J. H. Gibbs: J. chem. Phys., **43**, 139 (1965).

ACKNOWLEDGMENTS

The authors gratefully acknowledge the financial supports from the Engineering and Physical Science Research Council (EPSRC) for the grants (GR/M08127) and (GR/M29795) and from the European Office of Aerospace Research and Development (EOARD) in London (Ref. F61775-98-WE113).

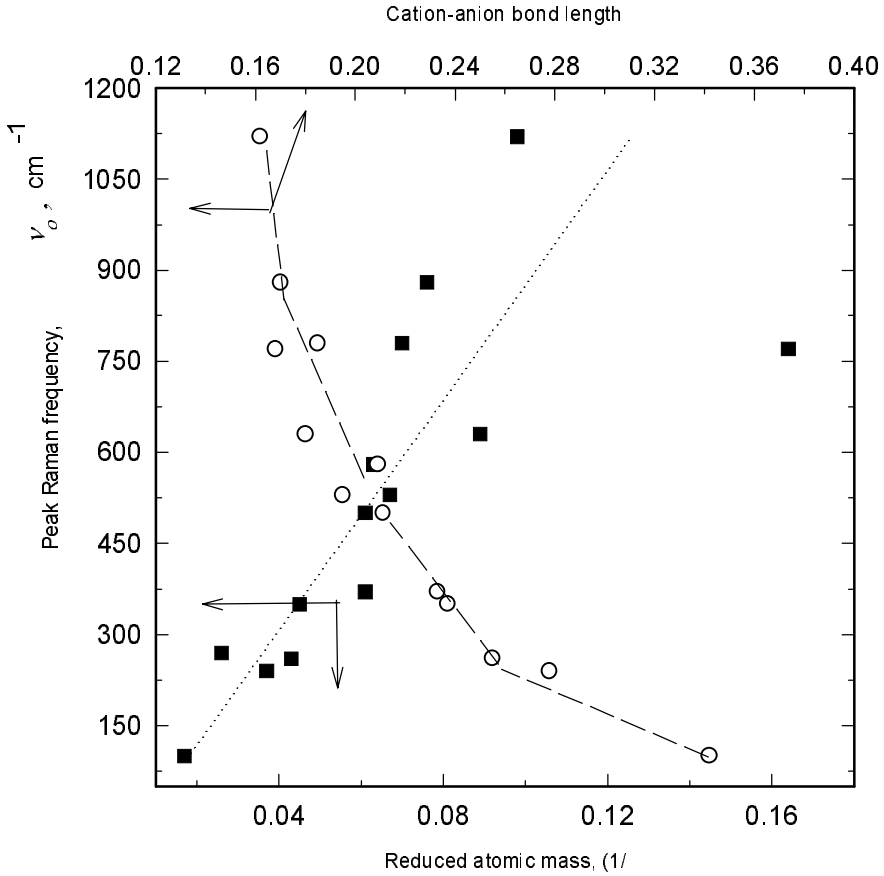

Figure 1: Relationships between the reduced mass (μ) and fundamental frequency of vibration, and interionic distance.

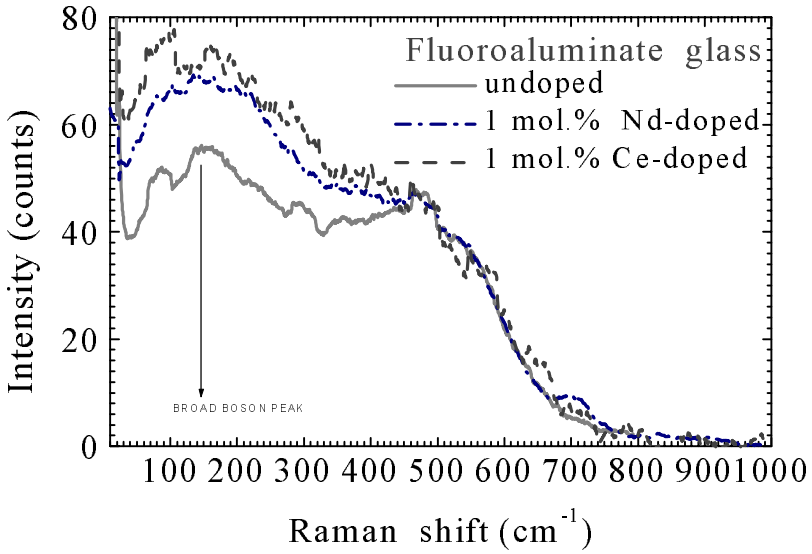

Figure 2a: Comparison of Boson peaks in undoped and rare-earth ion doped aluminium fluoride glasses

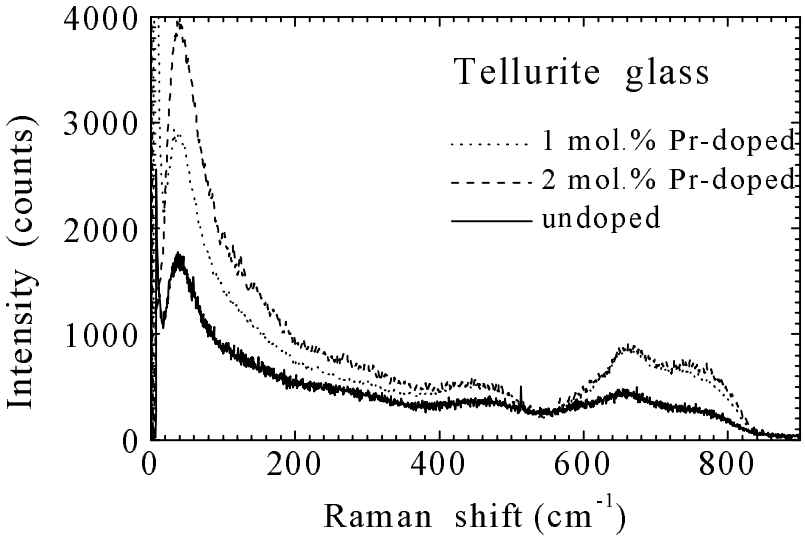

Figure 2b: Enhancement in the intensity of Boson peaks in Pr-doped TeO_2 Glasses.

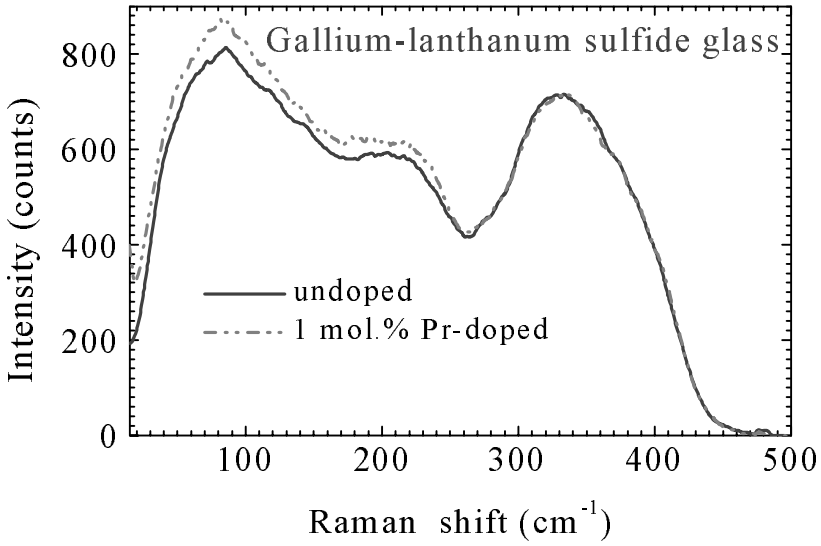

Figure 2c: Comparison of BP intensity in Gallium-lanthanum sulphide glasses

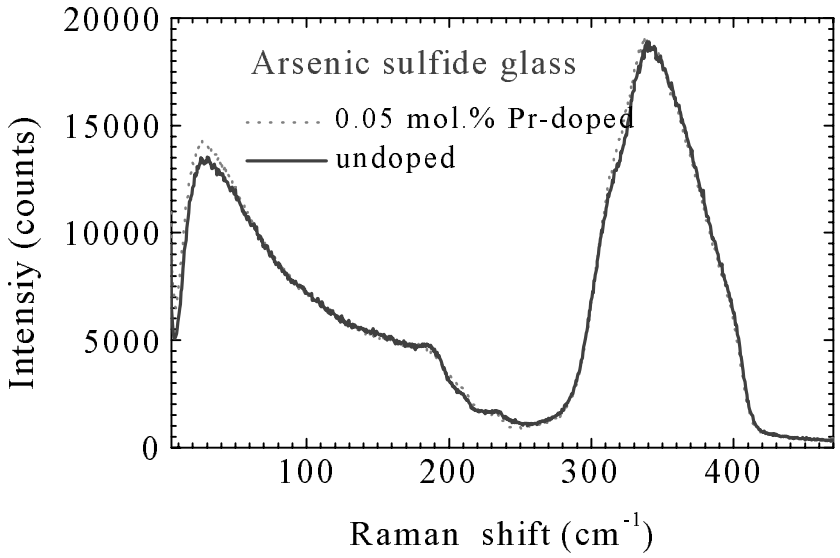

Figure 2d: Marginal enhancement in the intensity of BP in As_2S_3 glasses

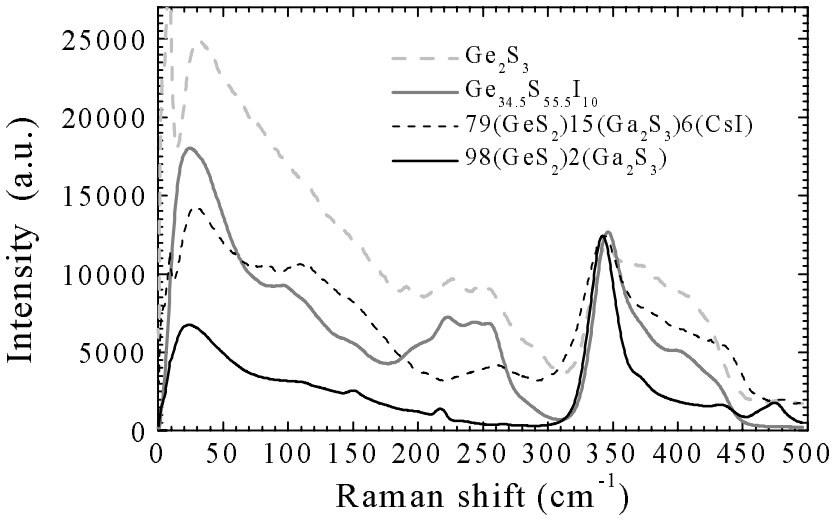

Figure 2e: Comparison of BP intensities as a function of glass composition.

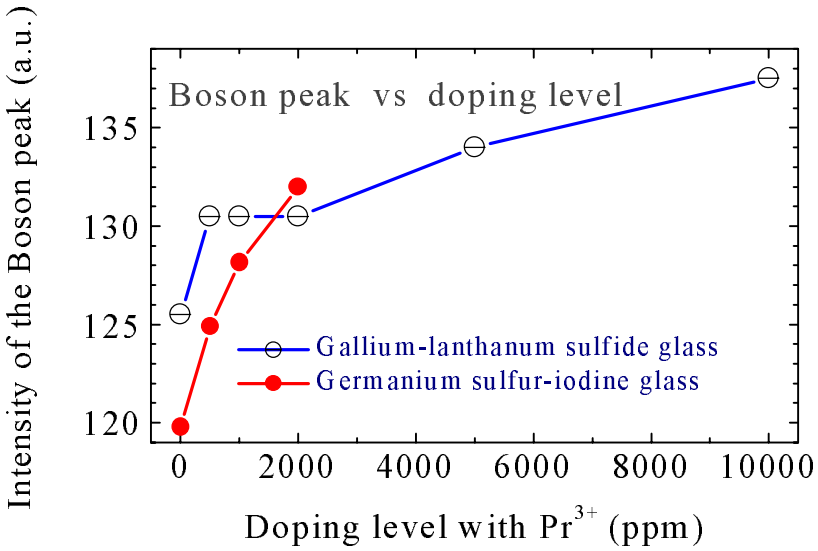

Figure 2f: A comparison of the influence of dopant concentrations on the relative intensities of BPs in GLS and Ge-S-I glasses.

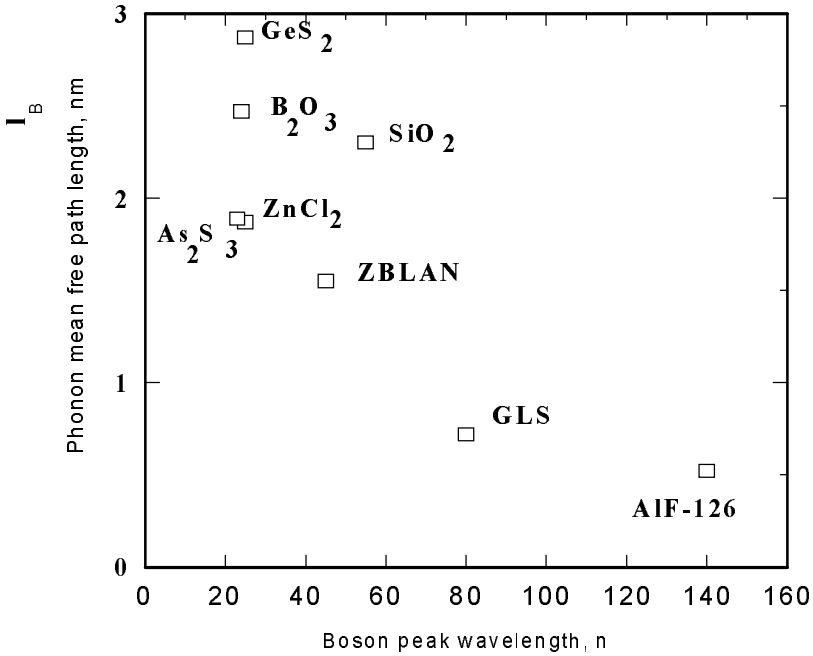

Figure 3 : A plot of phonon mean free path length and Boson peak wavelength for different glasses.

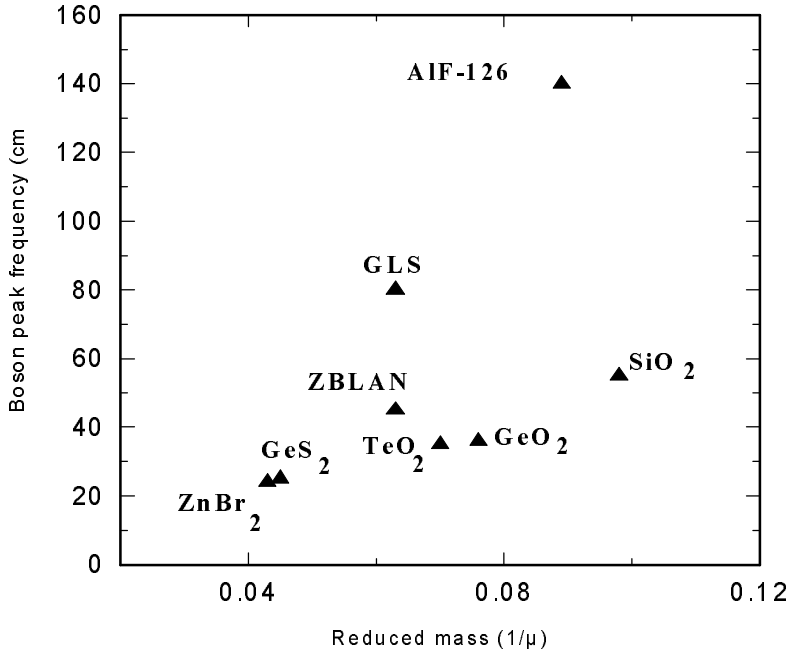

Figure 4 : A plot of Boson peak frequency against reduced mass, showing no linear relatioship as shown in eq.1.

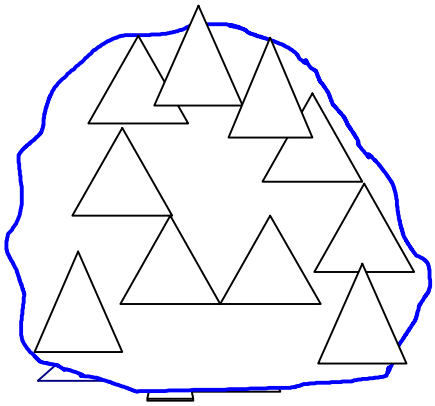

Figure 5 : Clustres of structural units (e.g. tetrahedra etc.) which sustain the acoustic phonon of wavelengths corresponding to l_B, nm.

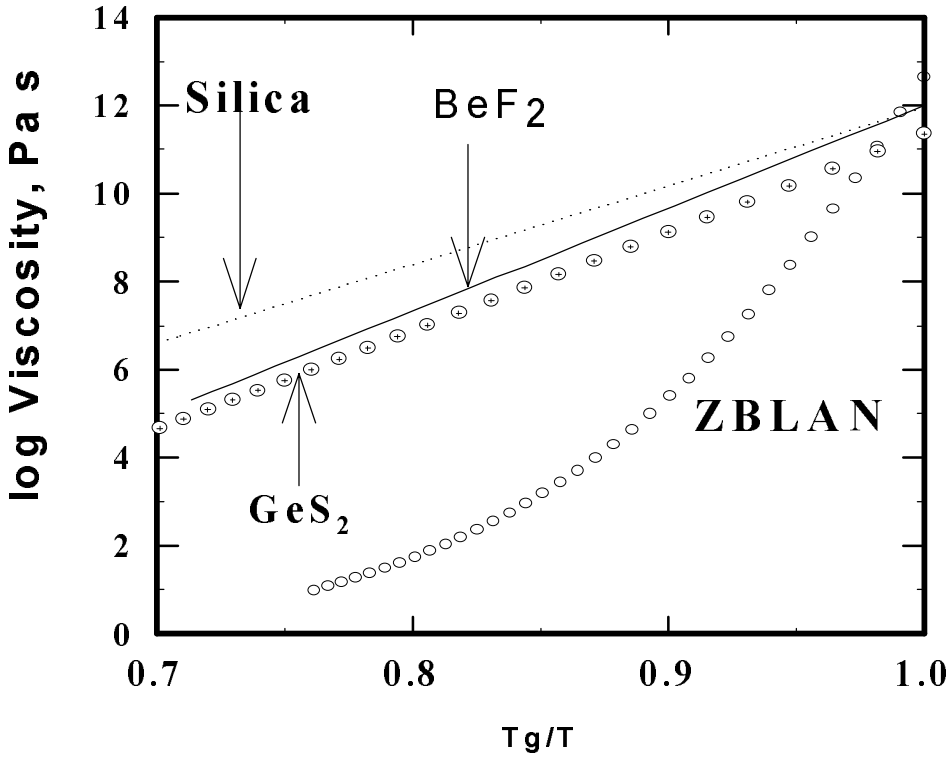

Figure 6: Viscosity versus !/T relationship for various glasses

Table 1: Glass compositions and their corresponding thermal, optical and spectroscopic properties.

Glass Names	T_g,K	R.I, IR and UV-visible edges			$\alpha.10^{-7}$ /°C
		n_D	λ_{IR}, μm	λ_{uv}, μm	
Silica (SiO_2)	1473	1.45	4.0	0.16	5.4
Germanate (GeO_2)	825-840	1.74	5-6.0	0.40	95
Tellurite, TeO_2	558	2.02	6.0	0.40	120
Ge-sulphide (Ge-1)	613-623	1.99	9.5	0.43	145
Ge-2	688	2.16	10.1	0.45	160
GLS	683	2.34	6.5	0.5-0.55	155
As_2S_3	470-478	2.45	10.2	0.80	185
BeF2	523	1.34	3.5	0.15	
ZBLAN	543	1.498	5.5	0.2-0.25	200
ALF-126	703	1.40	4.5-4.7	0.19	110
$ZnCl_2$	338	1.70	>9.0	0.32	
CBN-Ph	403	1.618	9.5	0.34	225
InF-1	565	1.498	8.5	0.29	183
InF-2	552	1.485	8.5	0.29	195
AgCsI	328	-	32	-	-

All compositions are given in mole percent (mol%).

1) Oxide glasses

Silica: 100 SiO_2, **Germanate**: 75 GeO_2, 25 Na_2O, **Tellurite**: 80 TeO_2, 10 ZnO, 10 Na_2O,

2) Sulphide glasses

Ge-1: 100 GeS_2, **Ge-2**: 79 GeS_2, 15 Ga_2S_3, 6 CsI, **GLS**: 70 Ga_2S_3, 30 La_2S_3, **As_2S_3:** 98 As_2S_3, 2 GeS_2.

3) Halide glasses

BeF_2: 100 BeF_2, **ZBLAN:** 50 ZrF_4, 20 BaF_2, 5 LaF_3, 5 AlF_3, 20 NaF

AlF-126: 30 AlF_3, (3.5 MgF_2, 20 CaF_2, 11 SrF_2, 13 BaF_2), 8.5 YF_3, 10 ZrF_4, 4 $NaPO_3$.

CBN-Ph: 50 CdF_2, 15 $BaCl_2$, 30 NaCl, 5 $NaPO_3$
$ZnCl_2$: 50 $ZnBr_2$-40KI-10$BaBr_2$
InF_3-1: 40 InF_3, 20 ZnF_2, 20 SrF_2, 17 BaF_2, 2 GaF_3, 1 LaF_3
InF_3-2: 36 InF_3, 20 ZnF_2, 20 BaF_2, 19 SrF_2, 4 GaF_3, 1 LaF_3
AgCsI: 55 AgI, 45 CsI.

Table 2: A comparison of data for the dominant Raman (ν_R) and Boson peaks (ν_B) in various glasses, their acoustic velocities (V_{ac}) and calculated Boson mean free path (l_B, nm).

Glass Name	ν_R, cm^{-1}	M^+-A^{n-}, nm	V_{ac}, ms^{-1}	ν_B, cm^{-1}	l_B, nm
SiO_2	1120[b]	0.162[b]	3800[a]	55[d]	2.3
GeO_2	880[b]	0.170[b]		36[b]	
B_2O_3	1500[b]	0.137[b]	1780[a]	24[a]	2.47
Tellurite	760, 660	0.185[b]		35	
Ge-S-I	350	0.220[b]	1750[a]	25	2.87
50 GeS_2 - 50 GeS	350	0.220[b]	1750[as1]	25	2.87
Ge-2	350, 420	0.220[b]	1750[as1]	25	2.87
98 GeS_2, 2 Ga_2S_3	480, 350	0.220[b]	1750[as1]	25	2.87
As_2S_3	340	0.228[b]	1400	25	1.87
70 Ga_2S_3 30 La_2S_3	350	0.246[est]	1750[as1]	80	0.72
ZBLAN	580[c]	0.209[c]	2100[a]	45[a]	1.55
ALF-126	620	0.180 (avg)	2100[as2]	140	0.52
50 $ZnBr_2$, 40 KI, 10 $BaBr_2$[a]	155, 144	0.232[b]	1300	23[a]	1.89

[a]: ref.19, [b]: ref.3, [c]: ref. 16, 23, [d]: ref.14
[est]: estimated from the ionic radii
[as1]: assumed to be same for all GeS_2 glasses
[as2]: assumed to be same as the ZBLAN glass

Table 3: The fitted viscosity equations, computed molar free volume at T_g derived from the Eyring hole theory equation [20,22]. Computed molar free volume (V_f) at T_g derived from viscosity and free volume equations and $\alpha_v.T_g = V_{tg}$ is the molar free volume at the onset of T_g.

Glass	$\log\eta$ = A + B/T Pa.s, **or** $\log\eta$ = A + B.exp(ß/T)	V_f	V_{tg}	$V_f - V_{tg}$
Silica	- 16.2 + 42,300/T	0.015	0.0123	0.0123
BeF_2	- 11.05 + 12,100/T	0.046	-	-
GeS_2	- 11.9 + 14800/T	0.039	0.022	0.017
CBN-Ph	8.5 + 2.6 exp (850/T)	0.150	0.028	0.122
ALF-126	- 5.3 + 0.22 exp(3200/T)	0.029	0.023	0.006
ZBLAN	$-1.43 + 8.6\times10^{-3}$. exp(3800/T)	0.029	0.025	0.0044
InF_3-1	- 0.54 + 0.034 exp(3400/T)	0.046	0.031	0.015